Secondary CD5+ Diffuse Large B-Cell Lymphoma Not Associated With Transformation of Chronic Lymphocytic Leukemia/Small Lymphocytic Lymphoma (Richter Syndrome)

Akiko Miyagi Maeshima, MD,[1] Hirokazu Taniguchi, MD,[1] Junko Nomoto, CT,[2] Dai Maruyama, MD,[2] Sung-Won Kim, MD,[2] Takashi Watanabe, MD,[2] Yukio Kobayashi, MD,[2] Kensei Tobinai, MD,[2] and Yoshihiro Matsuno, MD[3]

Key Words: CD5; Diffuse large B-cell lymphoma; Secondary disease; Immunohistochemistry; Non–Richter syndrome

DOI: 10.1309/AJCP58FETFGLCKKW

Abstract

Few cases of secondary CD5+ diffuse large B-cell lymphoma (DLBCL) that are not Richter syndrome have been reported previously. We report 9 cases of non–Richter syndrome secondary CD5+ DLBCL. Among 529 cases of DLBCL, 38 (7.2%) were CD5+ DLBCL, including 9 of secondary CD5+ DLBCL. Five cases gained CD5 expression during the clinical course of DLBCL (group 1). Three cases showed transformation from CD5– low-grade B-cell lymphoma to CD5+ DLBCL (group 2). The remaining case showed coexistence of CD5+ DLBCL and CD5+ follicular lymphoma. The clonal relationships of CD5– and CD5+ tumors were confirmed in all 4 available cases. Cases of secondary CD5+ DLBCL that were not Richter syndrome were classifiable into 3 groups. Groups 1 and 2 showed the gain of CD5 during the clinical course or transformation of the tumors, suggesting that CD5 expression is closely associated with the progression of B-cell lymphoma.

Diffuse large B-cell lymphoma (DLBCL) is the largest and most widely heterogeneous category of aggressive lymphomas.[1] CD5 expression in DLBCL is currently a focus of clinical and pathologic interest. Richter syndrome, transformation of chronic lymphocytic leukemia/small lymphocytic lymphoma (CLL/SLL), is a well-known form of secondary CD5+ DLBCL, but few cases of secondary CD5+ DLBCL that are not Richter syndrome have been reported previously.

The CD5 molecule is a 67-kDa glycoprotein that is expressed by most T cells and a subset of B cells.[2] Among mature B-cell neoplasms, most cases of CLL/SLL express CD5 and often undergo transformation to CD5+ DLBCL, so-called Richter syndrome. CD5 is also expressed in most cases of mantle cell lymphoma, but less frequently in DLBCL[3-5] and intravascular large B-cell lymphoma[6] and in only a small proportion of cases of extranodal marginal zone B-cell lymphoma,[7,8] Burkitt lymphoma,[9] follicular lymphoma (FL),[10-14] splenic marginal zone B-cell lymphoma,[15] and primary effusion lymphoma.[16] It is speculated that these neoplasms could switch or transform to CD5+ DLBCL, although few reports have indicated that CD5+ FL can transform to CD5+ DLBCL.[13,14] Moreover, apart from 1 case reported previously by our group,[17] transformation of CD5– low-grade B-cell lymphoma to CD5+ DLBCL seems to be rare.

Matolcsy et al[3] highlighted the phenomenon of de novo evolution of CD5 expression in DLBCL that is not a result of transformation, suggesting that such DLBCL is genotypically distinct from Richter syndrome–associated DLBCL. Yamaguchi et al[5] reported that CD5+ DLBCL accounted for approximately 10% of de novo DLBCL cases and that CD5 was a marker of poor prognosis in de novo DLBCL. They indicated that patients with CD5+ DLBCL showed an

older age distribution, a female predominance, poor performance status, a higher level of serum lactate dehydrogenase, advanced stage, a tendency to have more than 1 extranodal site and B symptom, and a higher International Prognostic Index score than patients with CD5– DLBCL. However, there has been no report of secondary CD5+ DLBCL gaining CD5 expression during the clinical course. Herein we report 9 cases of secondary CD5+ DLBCL that were not Richter syndrome.

Materials and Methods

Patient Selection

We reviewed the pathology archives of the National Cancer Center Hospital, Tokyo, Japan, for the period between 2002 and 2007. The total number of patients with DLBCL with or without a low-grade B-cell lymphoma component was 529, and the total number of specimens available was 728 (1-5 per case). Clinical information was extracted from the medical records, and the Ann Arbor system was used for staging.

Morphologic Review

The materials were fixed in 10% neutral-buffered formalin overnight, embedded in paraffin, cut into sections 4 μm thick, and stained with H&E for routine histologic evaluation. All specimens were reviewed by 3 pathologists (A.M.M., H.T., and Y.M.) to confirm that the morphologic characteristics fulfilled the criteria for DLBCL in the 2001 World Health Organization classification of lymphoid neoplasms.[1] When a low-grade B-cell lymphoma component was detected in previous or synchronous specimens, its histologic features were also evaluated. DLBCL was subclassified as the centroblastic, anaplastic, immunoblastic, or T-cell/histiocyte-rich variant. The presence of intravascular involvement, like that seen in intravascular large B-cell lymphoma, was also evaluated.

Immunohistochemical Studies, In Situ Hybridization, Flow Cytometry, and Interface Fluorescence In Situ Hybridization

We performed immunohistochemical analysis on formalin-fixed paraffin-embedded tissue samples by using a panel of monoclonal and polyclonal antibodies. Sections 4 μm thick were cut from each paraffin block, deparaffinized, and incubated at 121°C in citrate buffer, pH 6.0, for 10 minutes for antigen retrieval. Antibodies included those against the following antigens: CD3 (PS1, ×25; Novocastra, Newcastle upon Tyne, England), CD5 (4C7, ×50; Novocastra), CD10 (56C6, ×50; Novocastra), CD20 (L26, ×100; DAKO, Glostrup, Denmark), CD23 (1B12, ×100; Novocastra), bcl-6 (polyclonal, ×50; DAKO, Kyoto, Japan), cyclin D1 (SP4, ×25; Nichirei, Tokyo), MUM1 (MUM1p, ×50; DAKO, Kyoto), and p53 (DO7, ×100; DAKO, Glostrup), using an autostainer with the standard polymer (DAKO Autostainer Plus, Glostrup, for CD3, CD5, CD10, CD23, and cyclin D1) or the labeled streptavidin-biotin method (BioGenex Autostainer, San Ramon, CA, for CD20 and p53) or manually by the standard avidin-biotin complex method (bcl-6 and MUM1).

Immunohistochemical analysis for CD3, CD20, and CD5 was performed in all DLBCLs. Immunoreactivity for CD5 was judged positive if more than 20% of the tumor cells were stained. In all specimens of CD5– and CD5+ lymphomas of secondary CD5+ DLBCLs, CD5 was restained by the avidin-biotin complex method simultaneously, and the reproducibility of CD5 expression was confirmed. When a DLBCL had a CD5+ phenotype, the cyclin D1– phenotype was examined. The CD5– DLBCL or CD5– low-grade B-cell lymphoma and CD5+ DLBCL components were stained for CD10, bcl-6, MUM1, CD23, and p53, as well as for CD3, CD20, CD5, and cyclin D1.

To classify each case as having a germinal center B-cell (GCB) phenotype or a non-GCB phenotype, a panel of 3 antigens (CD10, bcl-6, and MUM1) was used according to the protocol reported by Hans et al.[18] All immunohistochemical specimens were judged by one of us (A.M.M.) and confirmed by 2 others (H.T. and Y.M.). In situ hybridization (ISH) with Epstein-Barr virus–encoded RNA (EBER-1) probes (DAKO, Glostrup) was performed to detect possible EBV infection.

Flow cytometry was performed on a Beckman Coulter Epics XL-MCL instrument with System II software (Beckman Coulter, Fullerton, CA). Cells were stained with fluorescein isothiocyanate–labeled antibodies against CD20 (B-Ly1, DAKO, Glostrup) and phycoerythrin-labeled CD5 (DK23, DAKO, Glostrup). The total population of viable cells was gated using forward and right scatter. Double positivity of CD5 and CD20 was defined as 15% or more of the population expressing both markers. The results of flow cytometry and immunohistochemical analysis were compared, and their degrees of agreement were examined.

Interface fluorescence ISH analysis was optional and performed on sections 4 μm thick cut from each paraffin block. Judgment of the fusion gene was performed as described previously.[19] Dual-color LSI IGH Spectrum Green/LSI BCL2 Spectrum Orange Dual Fusion Translocation Probes (Vysis, Downers Grove, IL) were used to detect *IGH/BCL2* fusion.

Polymerase Chain Reaction and Sequencing

DNA was extracted from paraffin-embedded tissue sections by using the DNA Micro Kit (Qiagen, Tokyo). To amplify the rearranged immunoglobulin heavy chain variable region gene, *CDR3,* we performed seminested polymerase chain reaction (PCR) using primers directed at consensus sequences of framework 3 (Fr3A, 5′-ACA CGG C(C/T)(G/C) TGT ATT ACT GT-3′) of the variable region and common sequence of the joining region (LJH, 5′-TGA GGA GAC

DOI: 10.1309/AJCP58FETFGLCKKW

GGT GAC C-3′ and VLJH, 5′-GTG ACC AGG GTN CCT TGG CCC CAG-3′). All PCR reactions were performed in 20-μL total volumes under standard conditions using LA *Taq* polymerase (Takara Bio, Shiga, Japan).

The amplified products were electrophoresed on 3% polyacrylamide gels. In cases with a monoclonal band, PCR products were purified by using Microcon YM-100 (Millipore, Bedford, MA). PCR amplification was performed by using the BigDye Terminator Cycle Sequencing Kit (Applied Biosystems, Foster City, CA), and automated fluorescent sequencing was performed on an ABI prism 310-Avant Genetic Analyzer (Applied Biosystems).

Results

Characteristics of Patients With Non–Richter Syndrome Secondary CD5+ DLBCL

There were 38 cases of CD5+ DLBCL (7.2%), among which 9 cases of secondary CD5+ DLBCL were identified (9/38 [24%]). None of the cases was Richter syndrome. Clinical information is summarized in ▮Table 1▮. The patients comprised 6 men and 3 women, ranging in age from 24 to 76 years with a median age of 63 years. Six patients had stage I or II disease, and 3 had stage III or IV disease at initial diagnosis. All patients received chemotherapy (cyclophosphamide, doxorubicin, vincristine, and prednisone or other types of regimen). The 5-year overall survival from initial diagnosis was 80%.

Three Histologic Groups of Secondary CD5+ DLBCL

The 9 cases of non–Richter syndrome secondary CD5+ DLBCL were classifiable into 3 groups. In the 8 cases constituting group 1 (gained CD5 expression during the clinical course of DLBCL, 5 cases) and group 2 (showed transformation from CD5– low-grade B-cell lymphoma to CD5+ DLBCL, 3 cases), the biopsy sites of CD5– B-cell non-Hodgkin lymphoma at initial diagnosis were lymph node (2), Waldeyer ring (1), and extranodal sites (5, 1 each in breast, bone marrow, maxillary sinus, orbit, and small intestine). The biopsy sites of the CD5+ DLBCLs were lymph node (5), tonsil (1), and extranodal sites (2, 1 each in skin and soft tissue). The single tumor constituting group 3 (case 9) was obtained

▮Table 1▮
Patient Characteristics in 9 Cases of Secondary CD5+ Diffuse Large B-Cell Lymphoma

Case No./ Sex/Age (y)	Months After Diagnosis	Histologic Type	CD5*	Biopsy Site	PS	Stage	IPI	LDH (U/L)†	EN	B Symptoms	Postbiopsy Therapy/Response	Follow-up (mo)/ Outcome
1/F/62	0	DLBCL	–	Breast	0	I	LI	506	0	–	CHOP ×6 and RT, 40 Gy/CR	
	37	DLBCL	+	Cervical LN							R-C-MOPP ×6 and RT, 40 Gy/CR	
	56	DLBCL	+	Inguinal LN							R ×1 and ESHAP ×3	58/AWD
2/F/63	0	DLBCL	–	Maxillary sinus	0	II	L	146	1	–	CHOP ×6, IT ×3, and RT, 46 Gy/PR	
	7	DLBCL	+	Cervical LN							EPOCH ×1/PD; IVAC ×1, and CODOX-M ×2/PD; R ×3/NC	13/AWD
3/M/24	0	DLBCL	–	Waldeyer ring	0	II	L	127	1	–	R ×4, CHOP ×6, and RT, 40 Gy/CR	
	8	DLBCL	+	Soft tissue							IT, RT at 30 Gy, R ×5, and IVAC ×3/PR; BMT	24/DOD
4/M/63	0	DLBCL	–	Cervical LN	0	II	L	209	0	–	R-CHOP ×6 and RT, 40 Gy/CR	
	15	DLBCL	+	Inguinal LN							Auto-PBSCT	19/AWOD
5/M/66	0	DLBCL	NA	Abdominal LN	0	IV	HI	305	2	–	CHOP ×8/CR	
	48	DLBCL	–	Prostate							EPOCH ×4/CR	
	75	DLBCL	+	Skin							RT, 35 Gy, and R-C-MOPP	77/AWD
6/M/47	0	FL, grade 2	–	Small intestine	0	II	L	150	1	–	CHOP ×8/CR; C-MOPP ×4 and RT, 40 Gy/CR	
	75	DLBCL	+	Tonsil							ESHAP ×3 + R ×8, R-ICE ×4	123/DOD
7/M/69	0	MALT lymphoma	–	Orbit	0	IV	H	439	2	–	R ×1, C-MOPP ×14, and VDS and C-MOPP ×6/PR	
	56	DLBCL	+	Abdominal LN								57/AWD
8/F/76	0	LPL	–	BM	2	IV	H	750	1	+	CHOP ×2/PD; R-ESHAP ×1/PR	
	0	DLBCL	+	Cervical LN								5/AWD
9/M/27	0	DLBCL and FL, grade 3b	+	Cervical LN	0	I	L	172	0	–	R ×8 , CHOP ×3 , RT, and 30 Gy/CR	2/AWOD

AWD, alive with disease; AWOD, alive without disease; BM, bone marrow; BMT, bone marrow transplantation; CHOP, cyclophosphamide, doxorubicin, vincristine, and prednisone; C-MOPP, cyclophosphamide, vincristine, prednisone, and procarbazine; CODOX-M, cyclophosphamide, doxorubicin, and high-dose methotrexate; CR, complete remission; DLBCL, diffuse large B-cell lymphoma; DOD, died of disease; EN, number of extranodal sites; EPOCH, doxorubicin, vincristine, etoposide, cyclophosphamide, and prednisone; ESHAP, etoposide, carboplatin, cytarabine, and methylprednisolone; FL, follicular lymphoma; H, high; HI, high intermediate; ICE, ifosfamide, carboplatin, and etoposide; IPI, International Prognostic Index; IT, intrathecal methotrexate and prednisolone; IVAC, ifosfamide, etoposide, and high-dose cytarabine; L, low; LDH, serum lactate dehydrogenase; LI, low intermediate; LN, lymph node; LPL, lymphoplasmacytic lymphoma; MALT, mucosa-associated lymphoid tissue; NA, not available; NC, no change; PBSCT, peripheral blood stem cell transplantation; PD, progressive disease; PR, partial remission; PS, performance status; R, rituximab; RT, radiotherapy; VDS, vindesine, doxorubicin, and prednisone.

* By immunohistochemical analysis.

† The reference range for all cases except case 5 is 119-229 U/L; for case 5, it is 260-420 U/L. Values are given in conventional units; to convert to Système International units (μkat/L), multiply by 0.0167.

from a lymph node. Table 1 and **Table 2** summarize the clinicopathologic findings.

The 5 cases in group 1 gained CD5 during the clinical course of DLBCL **Image 1**. CD5– DLBCL was the initial diagnosis presentation, and CD5 expression was 0% by immunohistochemical analysis. CD5+ DLBCL was the diagnosis at relapse, 7, 8, 15, 27, and 37 months after the initial diagnosis of CD5– DLBCL, respectively.

The 3 cases in group 2 gained CD5 throughout transformation of CD5– low-grade B-cell lymphoma to DLBCL. The initial diagnoses were CD5– FL grade 2, CD5– mucosa-associated lymphoid tissue (MALT) lymphoma, and CD5– lymphoplasmacytic lymphoma (LPL), and they transformed to CD5+ DLBCL. The case that showed transformation of CD5– FL to CD5+ DLBCL has been reported previously by our group.[17] Although this FL case had a CD10+/CD5– phenotype in an FL component and a CD10–/CD5+ phenotype in a DLBCL component, *IGH/BCL2* fusion was detected in both components, suggesting that transformation to CD5+ DLBCL had occurred. The patient with CD5– MALT lymphoma had stage IV disease at initial diagnosis, and, after 56 months, CD5+ DLBCL was diagnosed in an abdominal LN.

In the LPL case **Image 2**, multiple lymphoid cell aggregates with plasmacytoid differentiation were detected in a bone marrow aspiration specimen. This was diagnosed as low-grade B-cell lymphoma with plasmacytoid differentiation having a cytoplasmic IgM+ phenotype. The tumor extended to the general lymph nodes and bone marrow but involved no other sites, including the peripheral blood or spleen. The serum IgM level was high at 895 mg/dL. On the basis of this information, we diagnosed the disease as LPL. There was synchronous CD5+ DLBCL in the cervical lymph node.

The case constituting group 3 showed coexistence and gradual shift of CD5+/CD10+ FL grade 3b to CD5+/CD10+ DLBCL in the cervical lymph node.

Immunohistochemical Studies, ISH, and Clonality Analysis for Secondary CD5+ DLBCL

All specimens were negative for cyclin D1 by immunohistochemical analysis. CD10 and CD23 were both positive

Table 2
Results of Immunohistochemical, Flow Cytometry, FISH, EBER-1 ISH, and Clonality Analysis in 9 Cases of Secondary CD5+ DLBCL

Case No./ Histologic Subtype	CD20	CD5*	CD5†	Cyclin D1	CD10	CD23	bcl-6	MUM1	GCB/ Non-GCB	p53	EBER-1 ISH	FISH	Clonality
1													
DLBCL, centroblastic	+	– (0)	ND	–	–	–	ND	ND	ND	ND	ND	ND	Related
DLBCL, centroblastic	+	+ (20)	–	–	–	–	+	–	GCB	–	ND	ND	
DLBCL, centroblastic	+	+ (80)	+	–	–	–	+	–	GCB	–	–	ND	
2													
DLBCL, centroblastic	+	– (0)	ND	–	–	ND	ND	ND	ND	ND	ND	ND	ND
DLBCL, centroblastic	+	+ (100)	+	–	–	–	+	+	Non-GCB	ND	–	ND	
3													
DLBCL, centroblastic	+	– (0)	ND	–	–	–	–	+	Non-GCB	–	ND	ND	Related
DLBCL, centroblastic	+	+ (90)	+	–	–	–	–	+	Non-GCB	–	–	ND	
4													
DLBCL, centroblastic	+	– (0)	–	–	–	–	+	+	Non-GCB	–	ND	ND	ND
DLBCL, centroblastic	+	+ (60)	ND	–	–	–	+	+	Non-GCB	–	–	ND	
5													
DLBCL, centroblastic	+	ND	ND	ND	ND	ND	ND	ND	ND	ND	ND	ND	
DLBCL, centroblastic	+	– (0)	ND	–	–	–	+	+	Non-GCB	ND	ND	ND	Related
DLBCL, centroblastic	+	+ (80)	ND	–	–	–	+	+	Non-GCB	–	–	ND	
6													
FL, grade 2	+	– (0)	ND	–	+	–	ND	ND	GCB	ND	ND	IGH/BCL2 fusion +	ND
DLBCL, centroblastic	+	+ (100)	ND	–	–	–	ND	ND	ND	ND	ND	IGH/BCL2 fusion +	
7													
MALT lymphoma	+	– (0)	ND	ND	–	–	ND	ND	ND	–	ND	ND	ND
DLBCL, centroblastic	+	+ (80)	ND	–	–	–	ND	ND	ND	ND	ND	ND	
8													
LPL/BM	+	– (0)	–	–	–	–	–	+	Non-GCB	–	ND	ND	Related
DLBCL, centroblastic	+	+ (90)	ND	–	–	–	ND	ND	ND	–	ND	ND	
9													
DLBCL, centroblastic and FL, grade 3b	+	+‡ (100)	ND	–	+‡	+‡	+‡	+‡	GCB	ND	ND	IGH/BCL2 fusion –	

DLBCL, diffuse large B-cell lymphoma; EBER-1 ISH, Epstein-Barr virus–encoding RNA-1 in situ hybridization; FISH, interface fluorescence in situ hybridization; FL, follicular lymphoma; GCB, germinal center B-cell phenotype; LPL, lymphoplasmacytic lymphoma; MALT, mucosa-associated lymphoid tissue; ND, not done.
* By immunohistochemical analysis. Numbers in parentheses are the percentage of positive cells.
† By flow cytometry.
‡ Positive in the DLBCL and FL, grade 3b components.

DOI: 10.1309/AJCP58FETFGLCKKW

only in case 9, composite CD5+ DLBCL and FL grade 3b. Bcl-6 and MUM1 were positive in 5 of 6 CD5+ DLBCLs, and 2 were classified as the GCB phenotype and 4 as the non-GCB phenotype. p53 expression was less than 10% in all 5 cases tested. EBER-1 ISH was negative in all 5 cases tested. In all specimens (CD5– DLBCL, CD5– low-grade B-cell lymphoma, and CD5+ DLBCL) from 9 cases of secondary CD5+ DLBCL, CD5 was restained in parallel by the avidin-biotin complex method, and reproducibility of the CD5 expression (positive or negative result) was confirmed in all of them.

Paraffin-embedded tissue sections of CD5– and CD5+ tumors were available in 6 cases, and a total of 12 samples was applied to molecular analysis. Monoclonal rearrangements of the *CDR3* gene were detectable in 10 samples (83%), and sets of CD5– and CD5+ tumors were available for sequencing in 4 cases. The 2 tumors were clonally related in the 4 cases (Table 2).

Immunohistochemical Studies for CD5 Expression in 30 Patients With DLBCL Undergoing Sequential Biopsies

Transition of CD5 expression was examined by immunohistochemical analysis in 30 patients who underwent sequential biopsies among a total of 529 patients with DLBCL ▮Table 3▮. The number of sequential biopsies was 2 in 26 cases, 3 in 3 cases, and 5 in 1 case. The transition of CD5

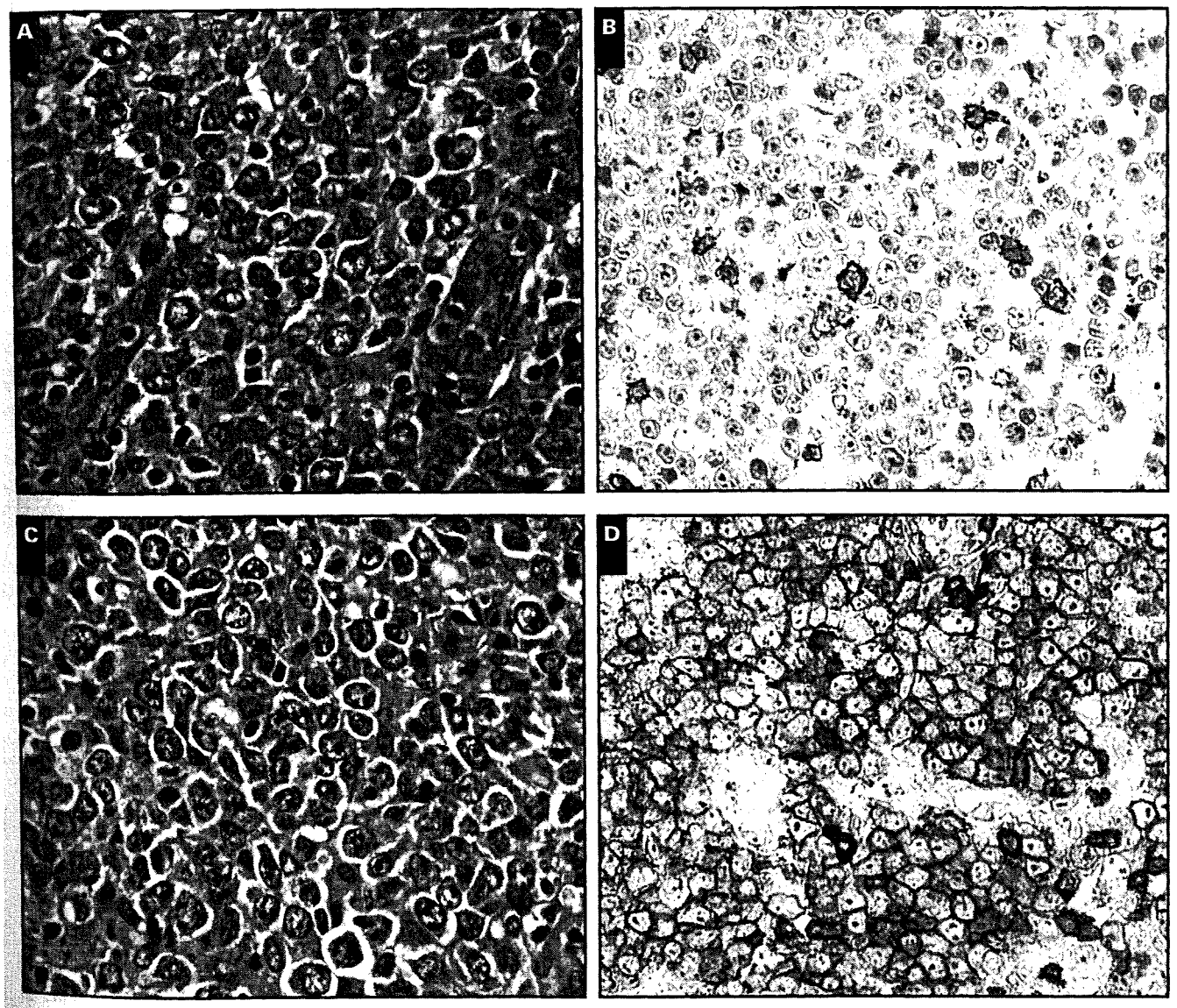

▮Image 1▮ (Case 4) Secondary CD5+ diffuse large B-cell lymphoma (DLBCL) derived from CD5– DLBCL. **A** and **B**, CD5– DLBCL in lymph node at initial diagnosis (**A**, H&E, ×400; **B**, CD5 by immunohistochemical analysis, ×400). **C** and **D**, CD5+ DLBCL in lymph node at relapse (**C**, H&E, ×400; **D**, CD5 by immunohistochemical analysis, ×400).

DOI: 10.1309/AJCP58FETFGLCKKW

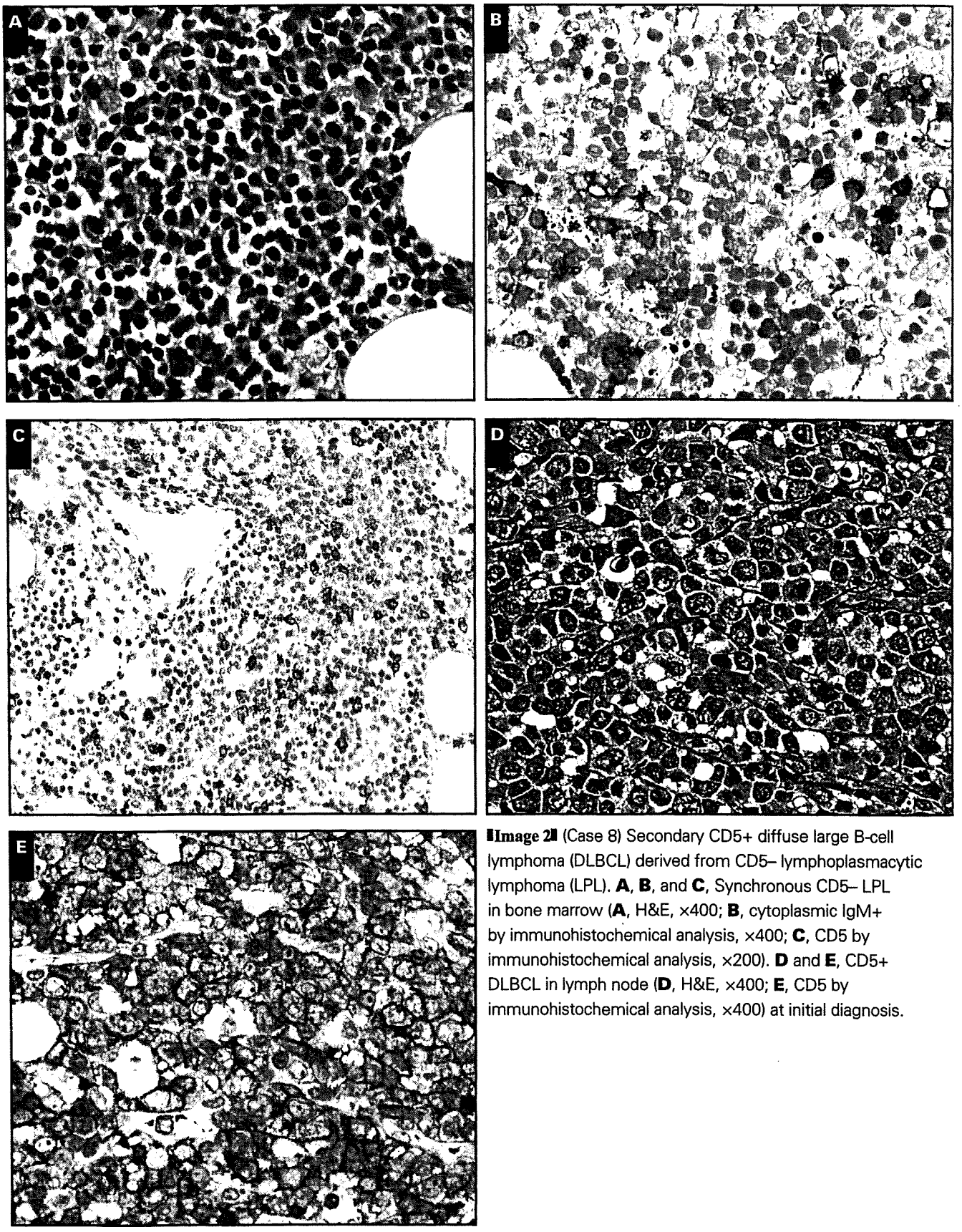

Image 2 (Case 8) Secondary CD5+ diffuse large B-cell lymphoma (DLBCL) derived from CD5– lymphoplasmacytic lymphoma (LPL). **A**, **B**, and **C**, Synchronous CD5– LPL in bone marrow (**A**, H&E, ×400; **B**, cytoplasmic IgM+ by immunohistochemical analysis, ×400; **C**, CD5 by immunohistochemical analysis, ×200). **D** and **E**, CD5+ DLBCL in lymph node (**D**, H&E, ×400; **E**, CD5 by immunohistochemical analysis, ×400) at initial diagnosis.

DOI: 10.1309/AJCP58FETFGLCKKW

expression was –/– in 20 cases, –/–/– in 2 cases, –/–/–/–/– in 1 case, –/+ in 4 cases, –/+/+ in 1 case, and +/+ in 2 cases; no case showed +/–.

Reproducibility of Data From Flow Cytometry and Immunohistochemical Studies in 89 DLBCLs

Among a total of 728 DLBCLs, flow cytometry results were available for 89 cases, and, therefore, the CD5 expression data obtained by immunohistochemical analysis and flow cytometry were compared. These results corresponded in 99% of the cases (88/89), including 83 cases with a CD5– phenotype and 5 cases with a CD5+ phenotype. The remaining case was CD5+ by immunohistochemical analysis and CD5– by flow cytometry.

Table 3
Transition of CD5 Expression in 529 Cases of DLBCL as Shown by Immunohistochemical Analysis*

Biopsy					
First	Second	Third	Fourth	Fifth	No. of Cases
–					464
–	–				20
–	–	–			2
–	–	–	–	–	1
–	+				4
–	+	+			1
+					35
+	+				2

DLBCL, diffuse large B-cell lymphoma.
* In 499 cases, 1 biopsy was done; in 30 cases, 2 or more biopsies were done.

Discussion

Among a total of 529 patients with DLBCL, 38 (7.2%) had CD5+ DLBCL. Probably because sequential biopsies were not infrequently performed at our institution, 9 cases (9/38 [24%]) of secondary CD5+ DLBCL were identified. All of them were non–Richter syndrome secondary CD5+ DLBCL. One of the most likely reasons for the lack of Richter syndrome cases in our series is that the frequency of CLL/SLL is very low in Japan compared with Western countries (1.3%).[20]

The 9 cases of non–Richter syndrome secondary CD5+ DLBCL were classifiable into 3 groups. Five cases constituting group 1 gained CD5 during the clinical course of DLBCL, and corresponded to 18% of patients (5/28) with DLBCL in whom sequential biopsies showed CD5– at the first biopsy. Thus, if rebiopsies are performed more frequently at relapse, more secondary CD5+ DLBCLs might be detected. The 3 cases constituting group 2 gained CD5 at the time of transformation from CD5– low-grade B-cell lymphoma. Except for our 1 reported case,[17] there has been no previous example of CD5– low-grade B-cell lymphoma transforming to CD5+ DLBCL. The sole case in group 3 showed a shift of CD5+ FL grade 3b to CD5+ DLBCL. Recently, it has been reported that CD5+ FL can transform to DLBCL.[13,14]

In the present study, we were unable to conclude that patients with non–Richter syndrome secondary CD5+ DLBCL had a poor outcome because the number of cases was small. However, group 1 and 2 tumors gained CD5 during the clinical course of CD5– DLBCL or transformation of CD5– low-grade B-cell lymphoma. Moreover, in 30 cases of DLBCL in which the patients underwent sequential biopsies, 5 showed a change of CD5 expression from negative to positive, but none changed from positive to negative. It was suggested that CD5 could be gained in association with tumor progression in DLBCL. This is in contrast with the fact that the B-chronic lymphocytic leukemia–specific markers CD5 and CD23 are frequently lost during transformation to DLBCL (Richter syndrome).[21] If some cases of non–Richter-syndrome secondary CD5+ DLBCL in group 1 or 2 had been included in previously reported de novo CD5+ DLBCL, it would have been consistent with the role of CD5 as a progression marker in de novo CD5+ DLBCL.

The frequency of CD5+ DLBCLs among the total DLBCLs in the present series was 7.2%, which was lower than the figure of 10% reported by Yamaguchi et al.[5] However, they performed immunohistochemical analysis on frozen tissue sections, whereas we used paraffin-embedded tissue sections, which could have led to false negativity. However, the high reproducibility of CD5 expression between flow cytometry and immunohistochemical analysis and between the polymer method and the avidin-biotin complex method of immunohistochemical analysis indicated that the CD5 expression data obtained by immunohistochemical analysis on paraffin-embedded tissues were not inferior to those obtained by flow cytometry. Therefore, we considered that the incidence of false negativity for detection of CD5 expression by immunohistochemical analysis on paraffin-embedded tissues was very low in DLBCLs.

Secondary CD5+ DLBCL was found to account for 24% of CD5+ DLBCL cases (9/38). Three groups of non–Richter syndrome secondary CD5+ DLBCL were identified and were shown to be derived from CD5– DLBCL, CD5– low-grade B-cell lymphoma, and CD5+ FL. In groups 1 and 2, CD5 was gained during the clinical course or transformation of tumors, suggesting that CD5 expression is closely associated with the progression of B-cell lymphoma.

From the [1]Clinical Laboratory and [2]Hematology and Stem Cell Transplantation Divisions, National Cancer Center Hospital, Tokyo, Japan; and [3]Department of Surgical Pathology, Hokkaido University Hospital, Sapporo, Japan.

Address reprint requests to Dr Maeshima: Clinical Laboratory Division, National Cancer Center Hospital, Tsukiji 5-1-1, Chuo-ku, Tokyo 104-0045, Japan.

Acknowledgments: We thank C. Kina and S. Miura for technical assistance with the immunohistochemical studies.

References

1. Harris NL, Ferry JA. Follicular lymphoma. In: Knowles DM, ed. *Neoplastic Hematopathology*. 2nd ed. Philadelphia, PA: Lippincott Williams & Wilkins; 2001:823-853.
2. Kipps TJ. The CD5 B cell. *Adv Immunol*. 1989;47:117-185.
3. Matolcsy A, Chadburn A, Knowles DM. De novo CD5-positive and Richter's syndrome-associated diffuse large B cell lymphomas are genotypically distinct. *Am J Pathol*. 1995;147:207-216.
4. Kroft SH, Howard MA, Picker LJ, et al. De novo CD5+ diffuse large B-cell lymphomas: a heterogeneous group containing an unusual form of splenic lymphoma. *Am J Clin Pathol*. 2000;114:523-533.
5. Yamaguchi M, Seto M, Okamoto M, et al. De novo CD5+ diffuse large B-cell lymphoma: a clinicopathologic study of 109 patients. *Blood*. 2002;99:815-821.
6. Murase T, Yamaguchi M, Suzuki R, et al. Intravascular large B-cell lymphoma (IVLBCL): a clinicopathologic study of 96 cases with special reference to the immunophenotypic heterogeneity of CD5. *Blood*. 2007;109:478-485.
7. Ferry JA, Yang WI, Zukerberg LR, et al. CD5+ extranodal marginal zone B-cell (MALT) lymphoma: a low grade neoplasm with a propensity for bone marrow involvement and relapse. *Am J Clin Pathol*. 1996;105:31-37.
8. Ballesteros E, Osbome BM, Matsushima AY. CD5+ low-grade marginal zone B-cell lymphomas with localized presentation. *Am J Surg Pathol* 1998;22:201-207.
9. Lin CW, O'Brien S, Faber J, et al. De novo CD5+ Burkitt lymphoma/leukemia. *Am J Clin Pathol*. 1999;112:828-835.
10. Tiesinga JJ, Wu CD, Inghirami G. CD5+ follicle center lymphoma: immunophenotyping detects a unique subset of "floral" follicular lymphoma. *Am J Clin Pathol*. 2000;114:912-921.
11. Barekman CL, Aguilera NA, Abbondanzo SL. Low-grade B-cell lymphoma with coexpression of both CD5 and CD10: a report of 3 cases. *Arch Pathol Lab Med*. 2001;125:951-953.
12. Barry TS, Jaffe ES, Kingma DW, et al. CD5+ follicular lymphoma: a clinicopathologic study of three cases. *Am J Clin Pathol*. 2002;118:1051-1057.
13. Catherwood MA, Venkatraman L. Follicular origin of a subset of CD5+ diffuse large B-cell lymphomas [letter]. *Am J Clin Pathol*. 2006;125:954-955.
14. Vasallo J, Bousquet M, Quelen C, et al. CD5-positive diffuse large B-cell lymphoma arising from a CD5-positive follicular lymphoma. *J Clin Pathol*. 2007;60:573-575.
15. Miyawaki S, Machii T, Hirabayashi H, et al. Splenic lymphoma with callous lymphocytes with CD5+, CD11c+ B-cell phenotype. *Intern Med*. 1993;32:472-475.
16. Fujisawa S, Tanioka F, Matsuoka T, et al. CD5+ diffuse large B-cell lymphoma with *c-myc/IgH* rearrangement presenting as primary effusion lymphoma. *Int J Hematol*. 2005;81:315-318.
17. Maeshima AM, Omatsu M, Nomoto J, et al. Diffuse large B-cell lymphoma after transformation from low-grade follicular lymphoma: morphological, immunohistochemical and FISH analyses. *Cancer Sci*. 2008;99:1760-1768.
18. Hans SP, Weisenburger DD, Greiner TC, et al. Conformation of molecular classification of diffuse large B-cell lymphoma by immunohistochemistry using a tissue microarray. *Blood*. 2004;103:275-282.
19. Sekiguchi N, Kobayashi Y, Yokota Y, et al. Follicular lymphoma subgrouping by fluorescence in situ hybridization analysis. *Cancer Sci*. 2005;96:77-82.
20. Lymphoma Study Group of Japanese Pathologists. The World Health Organization classification of malignant lymphomas in Japan: incidence of recently recognized entities. *Pathol Int*. 2000;50:696-702.
21. Mao Z, Quintanilla-Martinez L, Raffeld M, et al. IgV_H mutational status and clonality analysis of Richter's transformation. *Am J Surg Pathol*. 2007;31:1605-1614.

DOI: 10.1309/AJCP58FETFGLCKKW

Abdominal Imaging

Abdom Imaging (2009)
DOI: 10.1007/s00261-009-9516-9

Nodal status of malignant lymphoma in pelvic and retroperitoneal lymphatic pathways: PET/CT

Ukihide Tateishi,[1] Takashi Terauchi,[2] Tomio Inoue,[1] Kensei Tobinai[3]

[1]Department of Radiology, Yokohama City University Graduate School of Medicine, 3-9, Fukuura, Kanazawa-ku, Yokohama, Kanagawa 236-0004, Japan
[2]Division of Cancer Screening, Research Center for Cancer Prevention and Screening, National Cancer Center, Tokyo, Japan
[3]Hematology and Stem Cell Transplantation Division, National Cancer Center Hospital, Tokyo, Japan

Abstract

Nodal involvement of abdominal lymphatic pathways occurs in a number of histologic subtypes of malignant lymphoma. The histologic diagnosis of abnormal uptake in abdominal lymphatic pathways includes mainly non-Hodgkin lymphoma with B-cell lineage and Hodgkin lymphoma. Initial involvement of pelvic and retroperitoneal lymphatic pathways can result from a variety of underlying non-Hodgkin's lymphoma: follicular lymphoma, diffuse large B-cell lymphoma, marginal zone B-cell lymphoma of mucosa-associated lymphoid tissue (MALT) type, and mantle cell lymphoma. The diagnosis of these clinical entities requires various imaging techniques, including fluorine-18-fluorodeoxyglucose (^{18}FDG) positron emission tomography/computed tomography (PET/CT), computed tomography, ^{67}Gallium scintigraphy, and magnetic resonance imaging (MRI). Specific symptoms of these diseases are often lacking, but intense ^{18}FDG accumulation on PET/CT may be a marker of disease activity. Interpretation of the presence of and the specific pattern of ^{18}FDG uptake may obviate the need for invasive biopsy. However, distinction of abnormal uptake is often difficult to determine because focal accumulation of ^{18}FDG in the urinary tract or intestine mimics nodal involvement in the pelvic and retroperitoneal lymphatic pathways. In this review, specific conditions causing nodal involvement of pelvic and retroperitoneal lymphatic pathways in patients with malignant lymphoma that may impact diagnostic and treatment decisions are highlighted.

Correspondence to: Ukihide Tateishi; *email:* utateish@yokohama-cu.ac.jp

Published online: 16 April 2009

Key words: PET—PET/CT—Malignant lymphoma

Malignant lymphoma most often involves lymph nodes of pelvic and retroperitoneal lymphatic pathways at the initial staging. Nodal involvement within the pelvic or retroperitoneal lymphatic pathways results from disparate disease status. Tumor stage in malignant lymphoma is assessed initially by conventional imaging modalities such as positron emission tomography/computed tomography (PET/CT), PET, computed tomography (CT), magnetic resonance imaging (MRI), and ^{67}Gallium scintigraphy, which can play an important role in the initial determination of the stage because they provide morphologic information on the extent of disease. Fluorine-18 fluorodeoxyglucose (^{18}FDG) PET/CT or PET is a valuable tool for staging of patients with malignant lymphoma [1–3], therapeutic effect [4–7], and prediction of prognosis [8] in most histologic subtypes [9–13]. The anatomic location and specific features of ^{18}FDG accumulation often provide insights into disease activity and can sometimes explain occult disease progression. However, evaluation of pelvic or retroperitoneal nodal status with PET/CT can be complicated by urinary and intestinal activity or anatomic variants [14–16]. Discrete comparison with diagnostic contrast-enhanced CT study when evaluating PET/CT is often disturbed by misregistration, but contrast-enhanced PET/CT can improve anatomical localization of pelvic and retroperitoneal lesions. This review organizes the classification of malignant lymphomas involving pelvic and retroperitoneal lymph node, outlines anatomic distribution of pelvic and retroperitoneal lymph nodes, illustrates their PET/CT features, and summarizes method of detection.

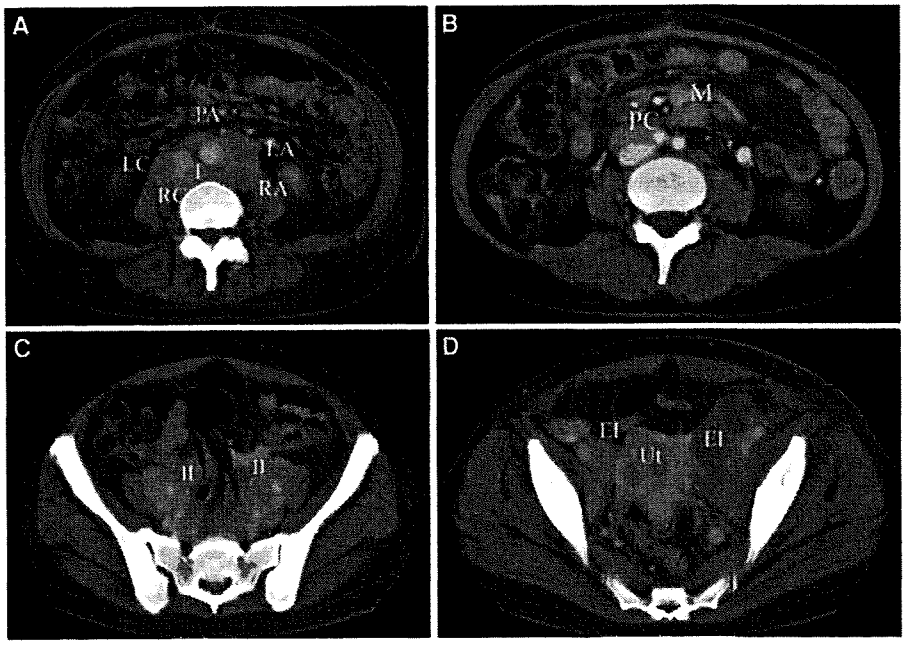

Fig. 1. **A–D** Axial contrast-enhanced CT image shows multiple enlarged lymph nodes in patient with follicular lymphoma. LA, lateroaortic lymph node; PA, preaortic lymph node; RA, retroaortic lymph node; LC, laterocaval lymph node; PC, precaval lymph node; RC, retrocaval lymph node; I, intermediate lumbar lymph node; M, mesenteric lymph node; II, internal iliac lymph node; EI, external iliac lymph node; Ut, uterus.

Imaging

The extent of disease does not necessarily correlate with the degree of ^{18}FDG accumulation; that is, some patients with ^{18}FDG-avid lymphoma show aggressive nature, whereas others with little avidity in the face of normal ^{18}FDG PET/CT may have systemic disease. Contrast-enhanced CT and ^{18}FDG PET have been sensitive for the detection of disease extent. However, contrast-enhanced CT and ^{18}FDG PET/CT are more sensitive and specific and are utilized for staging prior to therapy, re-staging after therapy or detection of recurrent disease, and the early recognition of therapeutic effect and clinical outcome [17–20].

Conventional CT

Conventional whole-body CT is routinely used for detection of lymphadenopathy. It is more preferable with a scan delay set at nearly 60 s after intravenous injection of contrast media. Although the detectability of lesions depends on slice thickness of standard reconstructed images which mostly ranges from 5.0 to 10.0 mm by means of a standard algorithm, nonmutually exclusive findings of lymphadenopathy may be seen: (1) enlarged lymph node greater than 10.0 mm in the axial plane and (2) enlarged lymph node with enhancement and its degree is greater than those of muscle and less than those of vessels (Fig. 1). Moreover, if an involved node is not enlarged greater than 10.0 mm, CT images may not reveal enough densities, especially when standard 7.0- or 10.0-mm-thick images are obtained. Conventional whole-body CT is performed prior to treatment and follow-up after treatment with a follow-up period usually at least every 3 or 6 months.

PET/CT

Because small involved lymph nodes are often misinterpreted as reactive lymph nodes on CT, ^{18}FDG PET/CT helps sort out equivocal cases. Generally, initial PET/CT is performed before therapy. Scans were acquired with PET/CT device that consisted of a PET scanner which had the theoretical spatial resolution and multislice CT scanner with a whole-body mode implemented as the standard software. Prior to the PET/CT study, the patients were fasted for at least 6 h. All patients were tested for a normal glucose level (range, 80–120 mg/dl) before ^{18}FDG administration. At first, noncontrasted CT for attenuation correction was performed from the head to the mid-thigh according to a standardized protocol with the following setting. Emission scans from the base of the skull to the mid-thigh were then obtained at about 60 min after the intravenous administration of ^{18}FDG.

Noncontrasted PET/CT can improve accuracy of staging compared with PET alone or diagnostic contrast-enhanced CT alone in patients with malignant lymphoma. However, the use of intravascular contrast material has an additional diagnostic impact in nodal staging of malignant lymphoma. After PET acquisition of 2–5 min per table position, contrast-enhanced CT was performed for the purpose of contrast-enhanced PET/CT from the head to the mid-thigh according to the same protocol as those

of CT without contrast enhancement. A total of 100 ml contrast material is administered intravenously using an autoinjector with a rate of 2.0 ml/s. Scan delay is set at 50–60 s after injection of contrast media [21–23].

Anatomic distribution of pelvic and retroperitoneal lymph nodes

The lymphatic pathway of pelvic organs drains either to visceral lymph nodes or regional nodes. The iliac lymph nodes consist of three different chains: right or left medial, intermediate, and right or left lateral (Table 1). The main channel which is often observed in iliac lymph nodes depends on nodal station and accompanying blood vessels. The main channel of the common iliac lymph node is the lateral chain. However, the main channel of the internal or external iliac lymph node is the medial chain. Recognition of the main channel in each lymph node is important for staging diagnosis because lymph nodes of the main channel are mostly involved in malignant lymphoma.

Retroperitoneal lymphatic pathway possesses different drainage areas from intraperitoneal lymphatic pathway. Retroperitoneal lymph nodes drain mainly to the lumbar lymph nodes, e.g., retrocaval lymph nodes, precaval lymph nodes, laterocaval lymph nodes, and intermediate lumbar lymph nodes (Table 1). The efferent lymph vessels from lumbar lymph nodes link to the thoracic duct together with the intestinal lymphatic trunk which includes mesenteric lymph nodes draining small and large intestine and the pelvic chain.

Table 1. Lymphatic pathway adjacent to urinary tract

Lymph node station	Laterality	
Lumbar lymph node		
Retrocaval lymph node	Rt	Lt
Precaval lymph node	NA	
Laterocaval lymph node	Rt	
Intermediate lumbar lymph node	NA	
Retroaortic lymph node	Rt	Lt
Preaortic lymph node	Rt	Lt
Lateroaortic lymph node		Lt
Pelvic lymph node		
Common iliac lateral lymph node	Rt	Lt
Common iliac intermediate lymph node	NA	
Common iliac promontory lymph node	NA	
Sigmoid lymph node[a]		Lt
Juxtaintestinal lymph node[a]		Lt
Internal iliac lymph node	Rt	Lt
External iliac lymph node	Rt	Lt
Pararectal lymph node[a]	Rt	Lt
Laterovesical lymph node[a]	Rt	Lt
Retrovesical lymph node[a]	Rt	Lt
Parauterine lymph node[a]	Rt	Lt

[a]Rarely involved lymph nodes
NA, not available; Rt, right; Lt, left

Abnormal uptake in the pelvic and retroperitoneal lymph nodes

At the initial staging, the pelvic and retroperitoneal lymph nodes are mostly involved in patients with Hodgkin lymphoma and non-Hodgkin's lymphoma: follicular lymphoma, diffuse large B-cell lymphoma, marginal zone B-cell lymphoma of mucosa-associated lymphoid tissue (MALT) type, and mantle cell lymphoma [24–26]. Intensely increased, partially symmetric ^{18}FDG accumulation is noted in the areas of the pelvic and retroperitoneal lymphatic pathway correlating to areas of lymphadenopathy on CT. Lumbar lymph nodes including the retrocaval lymph node, intermediate lumbar lymph node, retroaortic lymph node, and lateroaortic lymph node are most frequently involved at the initial presentation (Fig. 2). Abnormal uptake is often significant continuously from the precaval or preaortic lymph nodes to superior mesenteric lymph nodes, pancreaticoduodenal lymph nodes, and juxtaintestinal lymph nodes in patients with follicular lymphoma of various grades (Fig. 3). The lateral and intermediate common iliac lymph nodes, internal lilac lymph nodes, and external iliac lymph nodes are mostly involved in any types of malignant lymphoma (Fig. 4). However, lymph nodes of the common iliac promontory are frequently involved in follicular lymphoma (Fig. 5). On the other hand, areas of increased tracer activity often do not correlate to any mass lesions on CT. These areas of uptake represent normal physiological variants: urinary and intestinal activity or anatomic variants. Focal uptake of the ureter presenting at the lateral common iliac area mimics nodal involvement (Fig. 6). Normal activity in the jejunum is often misinterpreted as abnormal uptake in the external iliac lymph nodes (Fig. 7).

Differentiation of abnormal uptake from normal physiological variants with contrast-enhanced PET/CT

Integrated contrast-enhanced PET/CT improves the diagnostic accuracy in evaluating nodal status of pelvic and retroperitoneal lymphatic pathways in patients with malignant lymphoma, particularly detects a nodal involvement in a group of iliac lymph nodes adjacent to the ureter. Morimoto and colleagues described 66 patients with malignant lymphoma who underwent both noncontrasted PET/CT and contrast-enhanced PET/CT [21]. Nodal stage of pelvic and retroperitoneal lymphatic pathways was correctly determined in 47 patients on noncontrasted PET/CT, whereas determination of lymph node involvement based on contrast-enhanced PET/CT was correctly staged in 52 patients. Difference in the accuracy of nodal status between noncontrasted PET/CT and contrast-enhanced PET/CT was significant by McNemar test (Fig. 8).

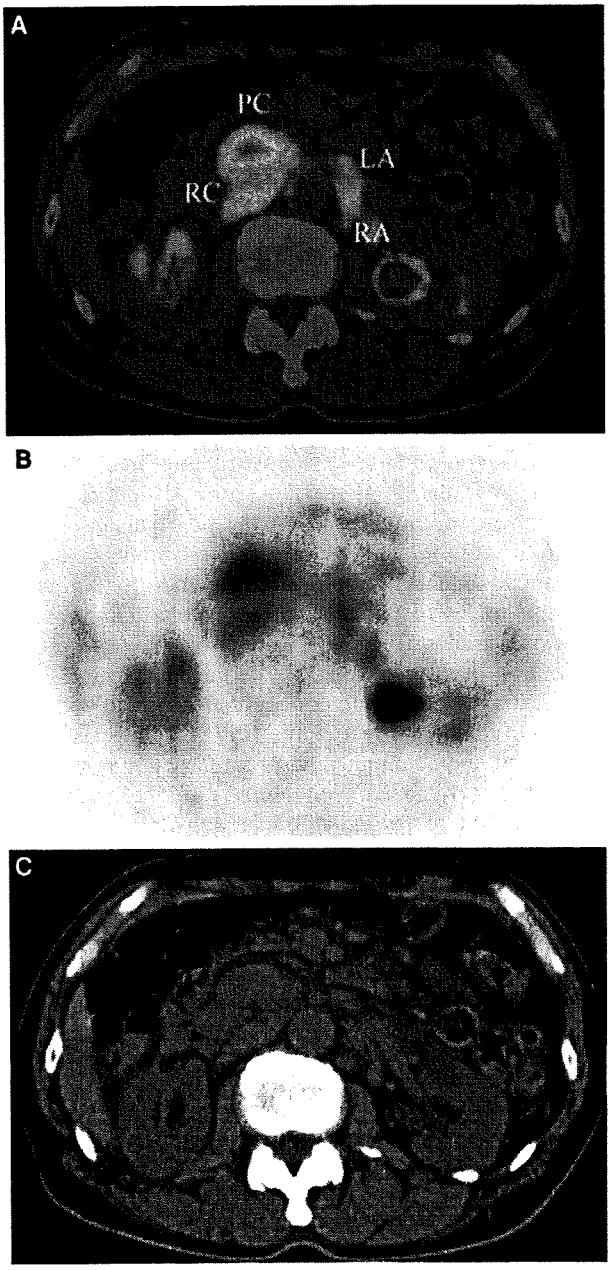

Fig. 2. Axial noncontrasted PET/CT image (**A**), PET (**B**), and CT (**C**) shows multiple enlarged nodes with increased uptake in patient with follicular lymphoma. LA, lateroaortic lymph node; RA, retroaortic lymph node; PC, precaval lymph node; RC, retrocaval lymph node.

Contrast-enhanced PET/CT determines the status of the common iliac lymph node, internal iliac lymph node, and external iliac lymph node more accurately than PET/CT. False-positive findings on contrast-enhanced PET/CT may be caused by misdiagnosing ureters or intestinal

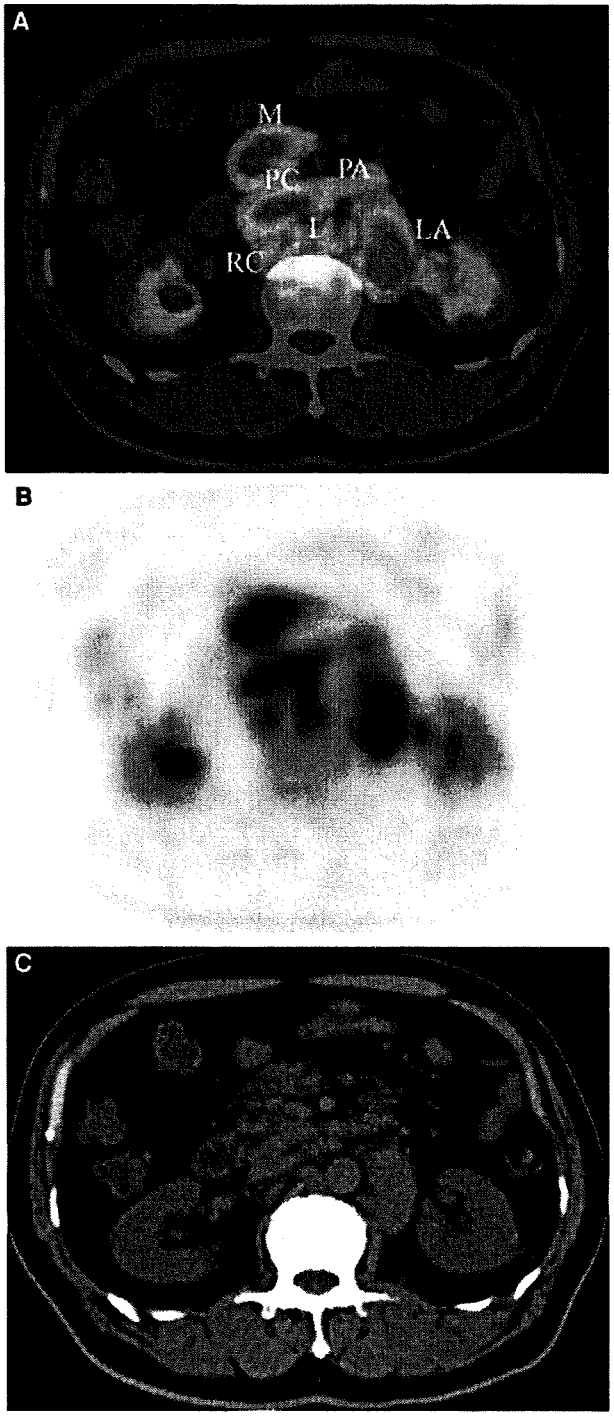

Fig. 3. Axial noncontrasted PET/CT image (**A**), PET (**B**), and CT (**C**) shows multiple enlarged nodes with increased uptake in patient with follicular lymphoma. LA, lateroaortic lymph node; PA, preaortic lymph node; PC, precaval lymph node; I, intermediate lumbar lymph node; RC, retrocaval lymph node; M, mesenteric lymph node.

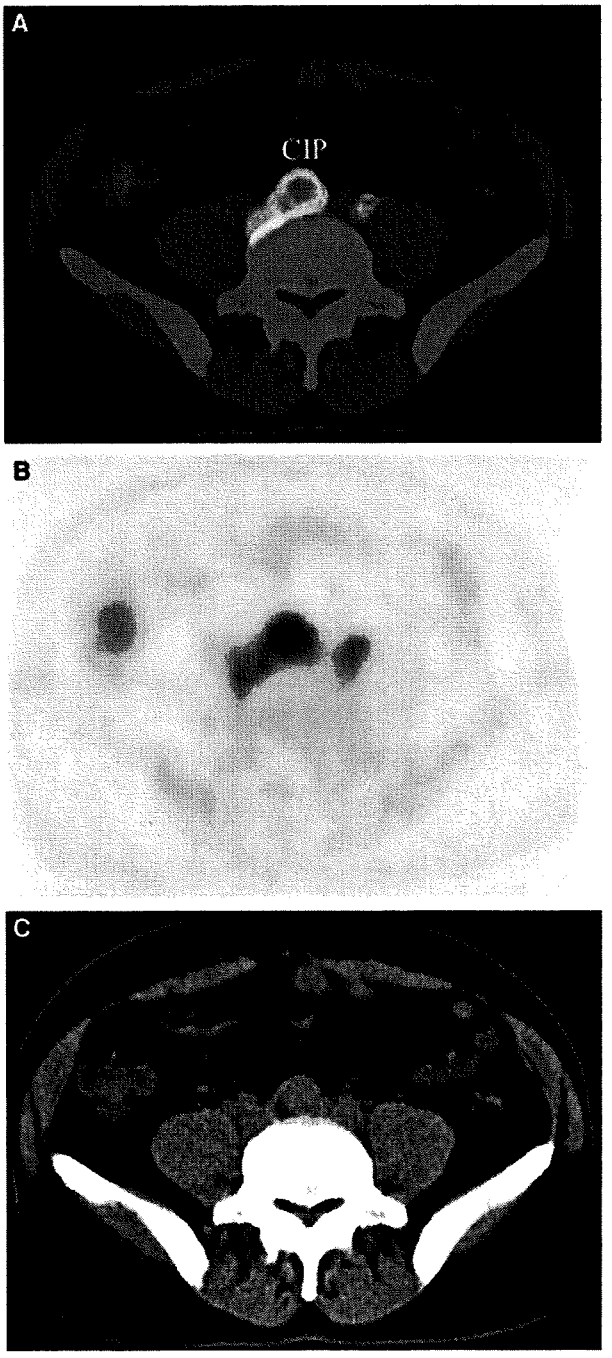

Fig. 4. Axial noncontrasted PET/CT image (**A**), PET (**B**), and CT (**C**) shows enlarged common iliac promontory (CIP) lymph nodes with increased uptake in patient with follicular lymphoma.

^{18}FDG uptake as lymph nodes. False-negative findings on contrast-enhanced PET/CT will be mainly due to involvement of subcentimeteric lymph nodes. However, diagnostic accuracies of lumbar lymph nodes: preaortic, lateroaortic, retroaortic, precaval, laterocaval, retrocaval, and intermediate lumbar nodes are similar by either noncontrasted PET/CT or contrast-enhanced PET/CT (Fig. 9). False-positive results in these nodes are often caused by misdiagnosing ureters as lymph nodes on both PET/CT with and without contrast enhancement. False-negative results of paraaortic and aortocaval lymph nodes are caused by intestinal ^{18}FDG uptake.

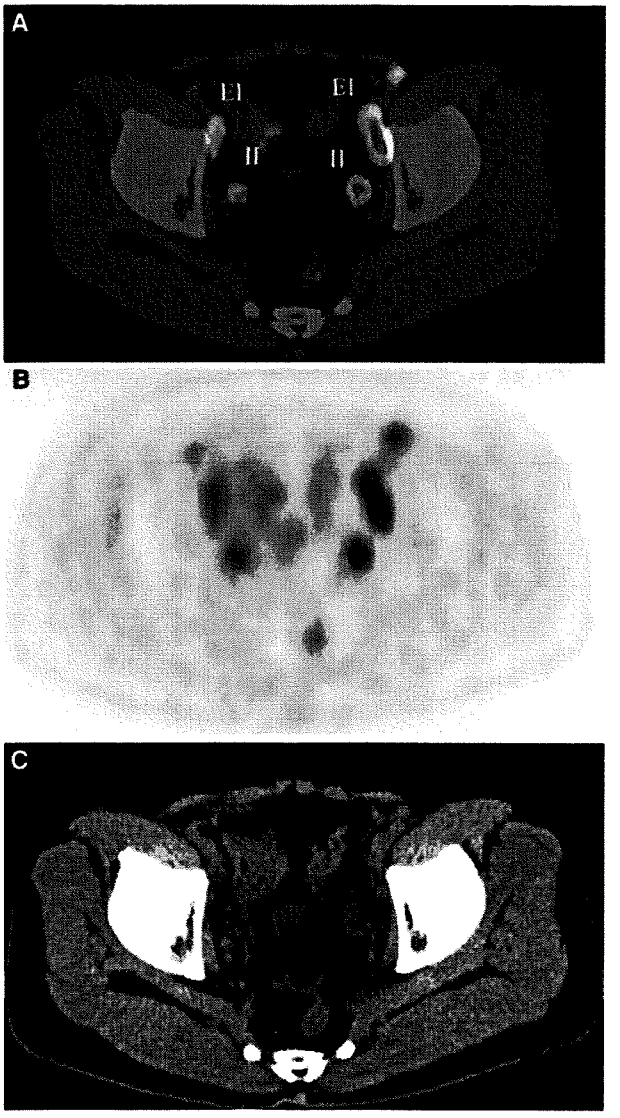

Fig. 5. Axial noncontrasted PET/CT image (**A**), PET (**B**), and CT (**C**) shows multiple enlarged nodes with increased uptake in patient with follicular lymphoma. II, internal iliac lymph node and EI, external iliac lymph node.

Clinical advantage by contrast-enhanced PET/CT

The lymphatic chains of the retroperitoneum and pelvis are complicated and numerous. Lymph nodes along the

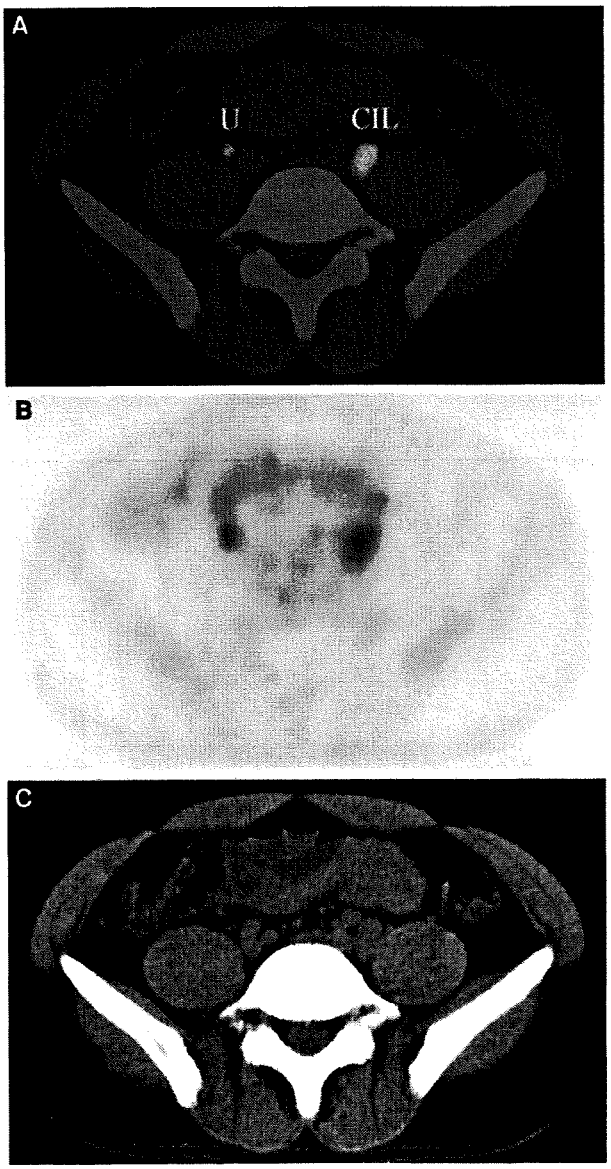

Fig. 6. Axial noncontrasted PET/CT image (A), PET (B), and CT (C) shows enlarged common iliac lateral lymph nodes with increased uptake in patient with follicular lymphoma. Focal uptake of ureter mimics abnormal uptake of common iliac lateral lymph node. CIL, common iliac lateral lymph node and U, ureter.

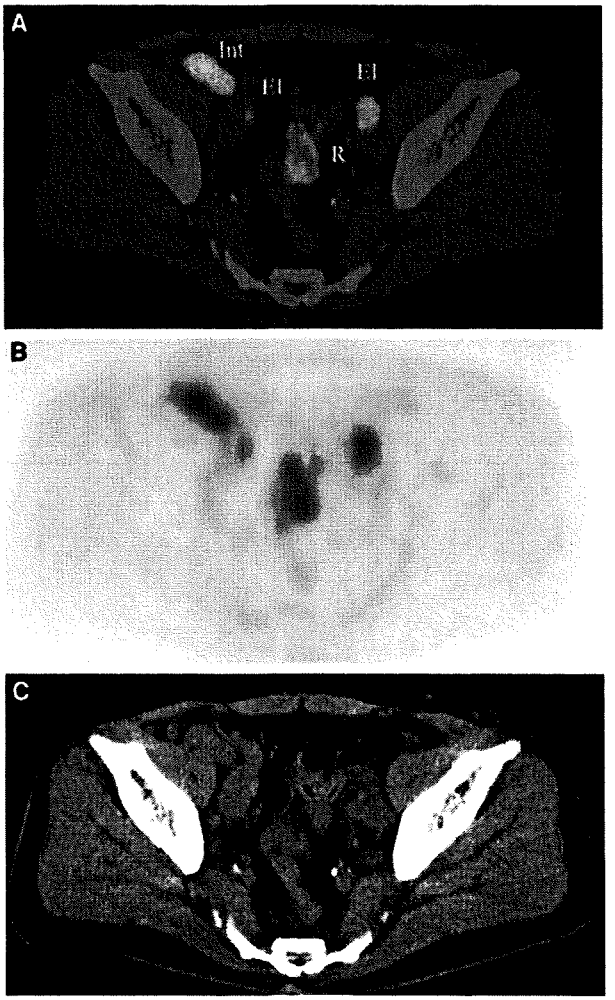

Fig. 7. Axial noncontrasted PET/CT image (A), PET (B), and CT (C) shows multiple enlarged nodes with increased uptake in patient with follicular lymphoma. Focal uptake of intestine (Int) mimics abnormal uptake of external iliac lateral lymph node. EI, external iliac lymph node and R, rectum.

pelvic and retroperitoneal lymphatic pathways are often identified at the initial presentation in patients with malignant lymphoma [27]. However, precise localization of lymph nodes in these regions is difficult only by noncontrasted images except for a bulky lesion. Contrast-enhanced PET/CT can reduce overstaged patients in number compared with noncontrasted PET/CT. In contrast, clinical stage will change from stage I or II to stage IV in patients who have a single focus along the pelvic and retroperitoneal lymphatic pathways. In addition, contrast-enhanced PET/CT depicts intravascular extension of tumor that cannot be diagnosed with noncontrasted PET/CT (Fig. 10). A recent study reported additional value of contrast-enhanced PET/CT compared with noncontrasted PET/CT in 47 patients with malignant lymphoma [23]. Diagnostic performance of two modalities is similar for initial staging with perfect correlation by Kappa statistics. However, unsuspected endometrial carcinoma and jugular thrombosis were identified only by contrast-enhanced PET/CT. Incidental findings, which often affect clinical outcome, will be observed by contrast-enhanced PET/CT.

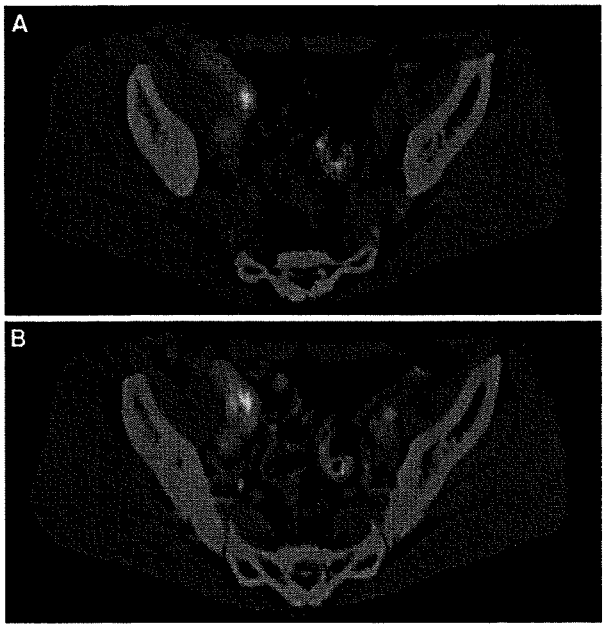

Fig. 8. Axial noncontrasted PET/CT image (**A**) and contrast-enhanced PET/CT (**B**) shows enlarged right internal iliac lymph node with increased uptake in patient with follicular lymphoma. Abnormal uptake is found in the right external iliac area on noncontrasted PET/CT, while this uptake corresponds to physiological uptake of jejunum on contrast-enhanced PET/CT.

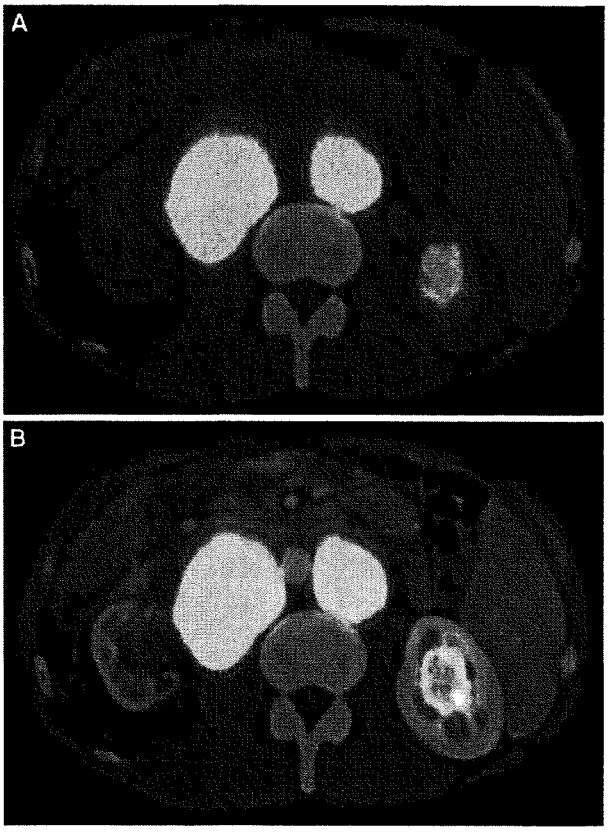

Fig. 9. Axial noncontrasted PET/CT image (**A**) and contrast-enhanced PET/CT (**B**) shows multiple enlarged lumbar lymph nodes with increased uptake in patient with follicular lymphoma. Delineation of the lesion is better on contrast-enhanced PET/CT.

Direct comparison of noncontrasted PET/CT and contrast-enhanced PET/CT

The advantage of using contrast-enhanced PET/CT is due to more accurate determination of lymph nodes along pelvic and retroperitoneal lymphatic pathways. Compared with noncontrasted PET/CT, contrast-enhanced PET/CT enabled more accurate staging, which results in an altered therapeutic plan. However, the diagnostic performance of PET/CT should be elucidated compared with standard contrast-enhanced CT in staging of malignant lymphoma. Tatsumi and colleagues performed a comparative study of PET and CT portion derived from PET/CT in 53 patients with malignant lymphoma [28]. Positive lesions identified by both modalities were mostly concordant by three physicians. However, 17% of 1,537 anatomic sites had discordant findings between PET and CT, and most of these lesions were truly positive by PET alone. The exact role of PET/CT in identification of a lesion will be provided by the PET portion of PET/CT which can differentiate undetermined lesions on CT. In contrast, Schaefer and colleagues conducted a prospective study comparing diagnostic accuracy between noncontrasted PET/CT and contrast-enhanced CT in 60 patients with malignant lymphoma [29]. Although diagnostic accuracies are different for evaluation of nodal or extranodal disease status, noncontrasted PET/CT is more accurate than contrast-enhanced CT in patients with malignant lymphoma. The study suggests that routine noncontrasted PET/CT should be performed at staging or restaging in malignant lymphoma instead of contrast-enhanced CT.

Influences of contrast agents on standardized uptake value (SUV)

Significant improvements in evaluating nodal status of pelvic and retroperitoneal lymphatic pathways are found with contrast-enhanced PET/CT. However, it should be clarified whether contrast media can affect SUV of the lesion in patients with malignant lymphoma. Vera and colleagues investigated quantitative evaluation of SUV on contrast-enhanced PET/CT in 50 patients with malignant lymphoma [22]. They found limited change of SUV (maximum 4%) on contrast-enhanced PET/CT compared with noncontrasted PET/CT before therapy and little change of SUV after therapy. Their results will

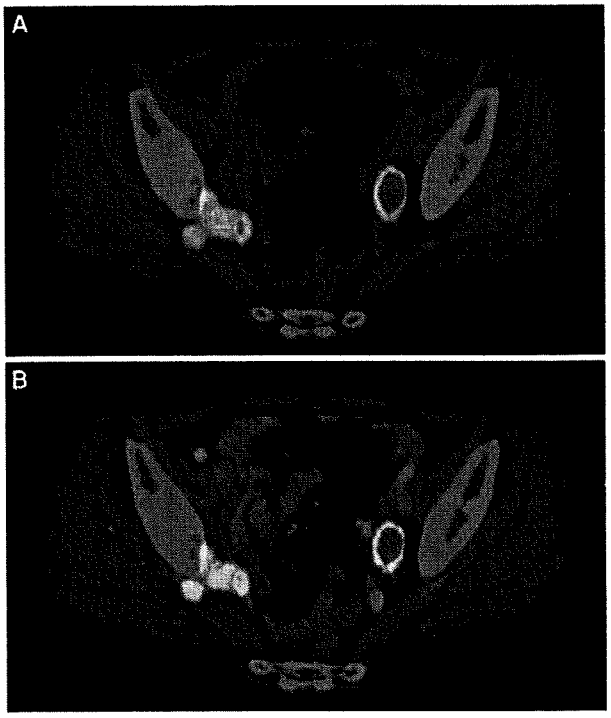

Fig. 10. Axial noncontrasted PET/CT image (**A**) and contrast-enhanced PET/CT (**B**) shows enlarged nodes with increased uptake in patient with follicular lymphoma. Abnormal uptake is found in the right gluteal lesion. Disappearance of right upper gluteal artery, which reflects intravascular extension, is also seen on contrast-enhanced PET/CT. Intense uptake is observed in the left hydroureter.

suggest that the difference of PET measurements by contrast-enhanced PET/CT is negligible and routine use of contrast-enhanced PET/CT is preferred for staging and follow-up in patients with malignant lymphoma.

Limitations

Despite the fact that noncontrasted or contrast-enhanced PET/CT improves the accuracy in staging or restaging in malignant lymphoma, the spatial resolution of PET/CT is not sufficient to detect small lymph nodes [30–32]. False-negative results are mainly due to small true-positive lymph nodes which are missed by PET/CT [18, 33–35]. On the other hand, main false-positive results are caused by misdiagnosis of physiological ^{18}FDG uptake as lymph node involvement. In the pelvic and retroperitoneal lymphatic pathways, urinary ^{18}FDG uptake often masks adjacent adenopathy by artifacts and makes lymph nodes less conspicuous [30–32]. A focal area of urinary uptake in ureter can also simulate nodal involvement. The proximal ureter parallels central retroperitoneal lymphatics and the distal third of the ureter lies in the extraperitoneal pelvis. The normal intestine commonly causes increased uptake of ^{18}FDG. Possible causes of ^{18}FDG uptake in the digestive tract are active smooth muscle, metabolically active mucosa, swallowed secretion, and colonic microbial uptake [30–32]. Intense FDG activity of the intestine can appear larger on PET/CT images than the actual size of the tracer collection. This phenomenon can affect assessment of retroperitoneal and pelvic lymph nodes.

Pathological examination for evaluating nodal status of pelvic and retroperitoneal lymph nodes which may be a cause of biased comparison is not performed routinely in the clinical setting. The cost effectiveness of contrast-enhanced PET/CT has not been fully elucidated. The relation between the benefit obtained by contrast-enhanced PET/CT and the risk of radiation exposure needs to be taken into account. The benefit–risk relationship between contrast-enhanced PET/CT and noncontrasted PET/CT should be clarified.

Conclusion

Nodal involvement of pelvic and retroperitoneal lymphatic pathways is often observed in patients with several histologic types of malignant lymphoma. These include Hodgkin lymphoma, follicular lymphoma, diffuse large B-cell lymphoma, marginal zone B-cell lymphoma of MALT type, and mantle cell lymphoma. Current diagnostic studies may be useful in revealing nodal status for purpose of staging or re-staging after treatment. Contrast-enhanced CT and noncontrasted PET/CT can detect typical involvement of each nodal station. Contrast-enhanced PET/CT is superior to standard staging method in detecting nodal involvement in a group of pelvic and retroperitoneal lymphatic pathways when these conditions are clinically suspected.

Acknowledgments. This work was supported in part by grants from Scientific Research Expenses for Health and Welfare Programs and the Grant-in-Aid for Cancer Research from the Ministry of Health, Labour and Welfare.

References

1. Jhanwar YS, Straus DJ (2006) The role of PET in lymphoma. J Nucl Med 47:1326–1334
2. Isasi CR, Lu P, Blaufox MD (2005) A metaanalysis of 18F-2-deoxy-2-fluoro-D-glucose positron emission tomography in the staging and restaging of patients with lymphoma. Cancer 104:1066–1074
3. Hicks RJ, Mac Manus MP, Seymour JF (2005) Initial staging of lymphoma with positron emission tomography and computed tomography. Semin Nucl Med 35:165–175
4. Podoloff DA, Macapinlac HA (2007) PET and PET/CT in management of the lymphomas. Radiol Clin North Am 45:689–696
5. Kumar R, Maillard I, Schuster SJ, Alavi A (2004) Utility of fluorodeoxyglucose-PET imaging in the management of patients with Hodgkin's and non-Hodgkin's lymphomas. Radiol Clin North Am 42:1083–1100
6. Burton C, Ell P, Linch D (2004) The role of PET imaging in lymphoma. Br J Haematol 126:772–784
7. Ulaner GA, Colletti PM, Conti PS (2008) B-cell non-Hodgkin lymphoma: PET/CT evaluation after 90Y-ibritumomab tiuxetan radioimmunotherapy—initial experience. Radiology 246:895–902

8. Hutchings M, Loft A, Hansen M, et al. (2006) FDG-PET after two cycles of chemotherapy predicts treatment failure and progression-free survival in Hodgkin lymphoma. Blood 107:52–59
9. Beal KP, Yeung HW, Yahalom J (2005) FDG-PET scanning for detection and staging of extranodal marginal zone lymphomas of the MALT type: a report of 42 cases. Ann Oncol 16:473–480
10. Karam M, Novak L, Cyriac J, et al. (2006) Role of fluorine-18 fluoro-deoxyglucose positron emission tomography scan in the evaluation and follow-up of patients with low-grade lymphomas. Cancer 107:175–183
11. Kumar R, Xiu Y, Zhuang HM, Alavi A (2006) 18F-fluorodeoxyglucose-positron emission tomography in evaluation of primary cutaneous lymphoma. Br J Dermatol 155:357–363
12. Tsai EY, Taur A, Espinosa L, et al. (2006) Staging accuracy in mycosis fungoides and sezary syndrome using integrated positron emission tomography and computed tomography. Arch Dermatol 142:577–584
13. Wohrer S, Jaeger U, Kletter K, et al. (2006) 18F-fluoro-deoxyglucose positron emission tomography (18F-FDG-PET) visualizes follicular lymphoma irrespective of grading. Ann Oncol 17:780–784
14. Ghersin E, Keidar Z, Eldad DJ, et al. (2007) Multimodality imaging of direct ureteric involvement in non-Hodgkin's lymphoma using PET/CT, CT urography and antegrade CT pyelography. Br J Radiol 80:e283–e286
15. Abouzied MM, Crawford ES, Nabi HA (2005) 18F-FDG imaging: pitfalls and artifacts. J Nucl Med Technol 33:145–155
16. Vesselle HJ, Miraldi FD (1998) FDG PET of the retroperitoneum: normal anatomy, variants, pathologic conditions, and strategies to avoid diagnostic pitfalls. Radiographics 18:805–823
17. von Schulthess GK, Steinert HC, Hany TF (2006) Integrated PET/CT: current applications and future directions. Radiology 238:405–422
18. Allen-Auerbach M, Quon A, Weber WA, et al. (2004) Comparison between 2-deoxy-2-[18F]fluoro-D-glucose positron emission tomography and positron emission tomography/computed tomography hardware fusion for staging of patients with lymphoma. Mol Imaging Biol 6:411–416
19. Freudenberg LS, Antoch G, Schutt P, et al. (2004) FDG-PET/CT in re-staging of patients with lymphoma. Eur J Nucl Med Mol Imaging 31:325–329
20. Raanani P, Shasha Y, Perry C, et al. (2006) Is CT scan still necessary for staging in Hodgkin and non-Hodgkin lymphoma patients in the PET/CT era? Ann Oncol 17:117–122
21. Morimoto T, Tateishi U, Maeda T, et al. (2007) Nodal status of malignant lymphoma in pelvic and retroperitoneal lymphatic pathways: comparison of integrated PET/CT with or without contrast enhancement. Eur J Radiol 67:508–513
22. Vera P, Ouvrier MJ, Hapdey S, et al. (2007) Does chemotherapy influence the quantification of SUV when contrast-enhanced CT is used in PET/CT in lymphoma? Eur J Nucl Med Mol Imaging 34:1943–1952
23. Rodríguez-Vigil B, Gómez-León N, Pinilla I, et al. (2006) PET/CT in lymphoma: prospective study of enhanced full-dose PET/CT versus unenhanced low-dose PET/CT. J Nucl Med 47:1643–1648
24. Even-Sapir E, Lievshitz G, Perry C, et al. (2007) Fluorine-18 fluorodeoxyglucose PET/CT patterns of extranodal involvement in patients with Non-Hodgkin lymphoma and Hodgkin's disease. Radiol Clin North Am 45:697–709
25. Bar-Shalom R (2007) Normal and abnormal patterns of 18F-fluorodeoxyglucose PET/CT in lymphoma. Radiol Clin North Am 45:677–688
26. Perry C, Herishanu Y, Metzer U, et al. (2007) Diagnostic accuracy of PET/CT in patients with extranodal marginal zone MALT lymphoma. Eur J Haematol 79:205–209
27. Macapinlac HA (2004) The utility of 2-deoxy-2-[18F]fluoro-D-glucose-positron emission tomography and combined positron emission tomography and computed tomography in lymphoma and melanoma. Mol Imaging Biol 6:200–207
28. Tatsumi M, Cohade C, Nakamoto Y, Fishman EK, Wahl RL (2005) Direct comparison of FDG PET and CT findings in patients with lymphoma: initial experience. Radiology 237:1038–1045
29. Schaefer NG, Taverna C, Strobel K, et al. (2007) Hodgkin disease: diagnostic value of FDG PET/CT after first-line therapy—is biopsy of FDG-avid lesions still needed? Radiology 244:257–262
30. Rodriguez-Vigil B, Gomez-Leon N, Pinilla I, et al. (2006) Positron emission tomography/computed tomography in the management of Hodgkin's disease and non-Hodgkin's lymphoma. Curr Probl Diagn Radiol 35:151–163
31. Strauss LG (1996) Fluorine-18 deoxyglucose and false-positive results: a major problem in the diagnostics of oncological patients. Eur J Nucl Med 23:1409–1415
32. Cook GJR, Fogelman I, Maisey MN (1996) Normal physiological and benign pathological variants of 18-fluoro-2-deoxyglucose positron emission tomography scanning: potential for error in interpretation. Semin Nucl Med 7:441–446
33. Hernandez-Maraver D, Hernandez-Navarro F, Gomez-Leon N, et al. (2006) Positron emission tomography/computed tomography: diagnostic accuracy in lymphoma. Br J Haematol 135:293–302
34. la Fougère C, Hundt W, Bröckel N, et al. (2006) Value of PET/CT versus PET and CT performed as separate investigations in patients with Hodgkin's disease and non-Hodgkin's lymphoma. Eur J Nucl Med Mol Imaging 33:1417–1425
35. Rhodes MM, Delbeke D, Whitlock JA, et al. (2006) Utility of FDG-PET/CT in follow-up of children treated for Hodgkin and non-Hodgkin lymphoma. J Pediatr Hematol Oncol 28:300–306

特集　リツキシマブ導入後のB細胞腫瘍治療

B細胞性リンパ腫とB細胞性慢性リンパ性白血病に対するベンダムスチンの有用性*

石澤賢一**

Key Words : bendamustine, chronic lymphocytic leukemia, indolent B-cell non-Hodgkin's lymphoma, mantle cell lymphoma, rituximab

はじめに

塩酸ベンダムスチンは構造的にアルキル化剤と代謝拮抗剤の特徴を有し，毒性が許容範囲内となるように設計された薬剤で，旧東ドイツのJenapharm社で合成され，1971年に旧東ドイツで販売が開始された．現在欧州ではドイツ，ブルガリアで低悪性度リンパ腫，慢性リンパ性白血病，骨髄腫を適応疾患として発売されている．米国では，2008年3月に慢性リンパ性白血病，同年10月にはリツキシマブ耐性低悪性度リンパ腫を適応として承認された．本邦でも，第I相試験，第II相試験が終了して，現在承認申請中である．

本剤はナイトロジェンマスタード基，プリン様ベンズイミダゾール基，酪酸側鎖の3つの部分で構成されている．ナイトロジェンマスタード基はcyclophosphamide, chlorambucil, melphalanと，酪酸側鎖はchlorambucilと共通である．またプリン様ベンズイミダゾール基は，プリン代謝拮抗剤のフルダラビン，クラドリビンと共通であり，これらを併せ持つユニークな構造は，既存の抗がん剤とは異なる作用機序が期待された[1]（図1）．事実，米国がん研究所のパネルスクリーニングによるコンペア解析では，cyclophosphamide, chlorambucil, melphalanでは相互に強い相関性が認められたが，これらのアルキル化剤と塩酸ベンダムスチンとの感受性の相関性は低く，既存のアルキル化剤とは異なる作用機序も有することが示唆された[2]．

これまで十分な質の高い臨床データが欠如していたこと，そのユニークな構造，作用機序より有効性，安全性の詳細な検討が必要であると考えられ，さまざまな条件下で臨床試験が実施された．

以下，低悪性度B細胞性リンパ腫，慢性リンパ性白血病に関して，その有効性，安全性を，主要な文献をもとに概説する．

低悪性度B細胞性リンパ腫に対する有効性，安全性

1．塩酸ベンダムスチン単剤の治療成績

(1)米国での第II相試験[3]

対象：再発，治療抵抗性低悪性度リンパ腫．単剤あるいは併用でのリツキシマブ投与歴があり，かつリツキシマブ抵抗性，あるいは不耐用と判断された症例．リツキシマブ抵抗性は，治療の反応しない，あるいは治療終了後6か月以内に病勢の進行を確認と定義された．

治療法：Day 1, 2 に塩酸ベンダムスチン120mg/m²を点滴静中．これを3週間ごとに病勢の進行が確認されない限り6コースを目標に，

* Efficacy of bendamustine in patients with chronic lymphocytic leukemia and B cell lymphoma.

** Kenichi ISHIZAWA, M.D., Ph.D.: 東北大学病院血液・免疫科〔〒980-8574 仙台市青葉区星陵町1-1〕; Department of Hematology & Rheumatology, Tohoku University Hospital, Sendai 980-8574, JAPAN

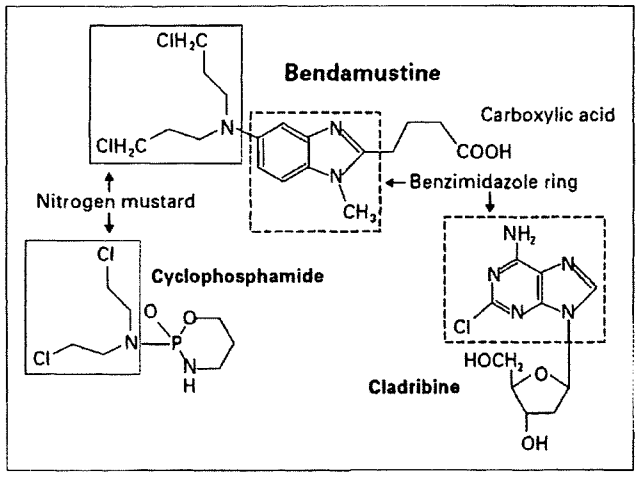

図1　塩酸ベンダムスチンの構造(文献[1]より引用改変)

治療効果が認められれば最大12コースまで投与するデザインで実施された.

症例数：期待全奏効率35%，閾値全奏効率20%として，目標症例数72症例.

結果：2003年9月から2005年2月まで，計77名が登録されたが1名が投与に至らず，解析対象は76名．年齢の中央値63歳(38～84歳)，前治療歴の中央値2レジメン(1～5レジメン)．組織学的進展例が15例含まれた.

実施コース数の中央値は5コース(1～9コース)で，目標の6コースを完遂できたのは34例(44%)であった．治療を6コース未満で中止した理由としては有害事象が23例で，そのうち血小板減少が最多で11例，原疾患の進行によるものが14例であった．放射免疫療法の治療歴がある9例中6例が血小板減少にて中止となり，減量が必要であったのは19例(25%)であった.

有害事象は血液毒性が主で，多くはグレード2以下が主であったが，グレード3以上の好中球減少が54%，血小板減少が25%認められた．非血液毒性では頻度順に悪心が72%，倦怠感が49%，嘔吐が41%認められたが，グレード3以上は倦怠感の7%が最多であった.

有効性は，全奏効率77%，完全寛解率34%．奏効持続期間の中央値は6.7か月で，組織型別の解析では，低悪性度リンパ腫で9.0か月，組織学的進展例で2.3か月．また観察期間の中央値26か月で，無増悪生存期間の中央値7.1か月．組織型別の解析では，低悪性度リンパ腫で8.3か月，組織学的進展例で4.2か月であった．アルキル化剤を含む化学療法で反応が認められなかった，あるいは増悪した23人の検討では，全奏効率61%で3例の完全寛解が確認された．またフルダラビン抵抗性8例の検討では，全奏効率は62%であった.

コメント：リツキシマブ抵抗例に対するベンダムスチンの有効性，安全性を前向きに評価した最初の試験である．高い奏効率が示され，有害事象も通常の支持療法で対応可能なレベルであり，単剤でも再発低悪性度リンパ腫治療において有力な選択肢となりうることが明らかになった．また少数例の検討ではあるが，アルキル化剤，プリン類似体抵抗例でも60%以上の全奏効率が得られており，米国でのコンペア解析の結果を*in vivo*で支持するものとなった．しかし低悪性度群と比較して，組織学的進展例での治療効果は明らかに劣っており，引き続き実施された第III相試験では対象から除外された.

(2)米国，カナダでの第III相試験[4]

対象：再発，治療抵抗性低悪性度リンパ腫で，組織学的進展例は除外し，1～3レジメンの化学療法の実施歴，単剤あるいは併用でのリツキシマブ投与歴があり，かつリツキシマブ抵抗性と判断された症例を対象とした．リツキシマブ抵

抗性は，リツキシマブ単剤4コース以上，リツキシマブ併用化学療法に反応しない，あるいは治療終了後6か月以内に病勢の進行，リツキシマブ維持療法中，終了6か月以内に病勢の進行が確認された症例と定義された．

治療法：Day 1, 2 に塩酸ベンダムスチン120mg/m²を点滴静中．これを3週間ごとに病勢の進行が確認されない限り，6～8コースを目標に投与するデザインで実施された．

症例数：期待全奏効率60%，閾値全奏効率40%として，目標症例数100症例．

結果：2005年10月から2007年7月まで，計102名が登録されたが2名投与に至らず，解析対象は100名．年齢の中央値60歳(31～84歳)，前化学療法歴の中央値2レジメン(0～6レジメン)．1例はリツキシマブ単剤のみで化学療法を受けておらず，8例は4レジメン以上の化学療法を受けていたため，プロトコル違反と判定されたが，解析対象とした．直近の化学療法に抵抗性であったのは36%．

実施コース数の中央値は6コース(1～8コース)で，目標の6コースを完遂できたのは60例(60%)．40例が治療6コース未満で中止となったが，その理由としては有害事象が27例(血小板減少9例，倦怠感6例など)，原疾患の進行によるものが10例．有害事象により減量が必要であったのは24%．全体では減量，投与延期，プロトコル中止となったのは68%であった．

有害事象は血液毒性が主で，グレード3以上の好中球減少が61%，血小板減少が25%，発熱性好中球減少は6%に認められた．非血液毒性は，悪心77%，感染症69%，倦怠感64%，下痢42%，嘔吐が40%認められた．グレード3以上が10%以上出現したものは，感染症21%，倦怠感14%であった．グレード4の感染症は6%であった．またCMV感染が5%認められた．過敏反応は14%認められた(表1)．

表1 ベンダムスチン単剤第III相試験の有害事象

有害事象	全グレード(%)	グレード3,4(%)
血液毒性		
貧血	94	10
血小板減少	88	25
好中球減少	83	61
発熱性好中球減少	6	6
非血液毒性		
悪心	77	4
感染	69	21
倦怠感	64	14
下痢	42	5
嘔吐	40	2
発熱	36	1
便秘	31	0

全グレードで20%以上． (文献[4]より引用改変)

有効性は，全奏効率75%，完全寛解率17%．病理組織別にみても，有効性に差はなかった(表2)．直近の化学療法に感受性あり(PR以上)の場合，全奏効率は88%，なしの場合は64%であった．またアルキル化剤を含む化学療法に感受性ありの場合，全奏効率は86%，なしの場合60%．治療奏効期間の中央値は9.2か月であった．また観察期間の中央値11.8か月で，無増悪生存期間の中央値7.5か月であった(図2)．アルキル化剤を含む化学療法に感受性ありの場合，無増悪生存期間の中央値は11.8か月，なしの場合7.5か月であった．

コメント：濃厚な治療歴を有する集団を対象に，全奏効率75%と，先に実施された第II相試験の結果が再現された．有効性に関しては本試験，安全性に関しては本試験と前述の第II相試験の結果を持って2008年10月，FDAはリツキシ

表2 ベンダムスチン単剤第III相試験の治療効果

	症例数	全奏効率(%)	CR+CRu(%)
全症例	100	75	17
病理組織別			
濾胞性リンパ腫	62	75	20
小リンパ球性リンパ腫	21	71	5
節性辺縁帯B細胞リンパ腫	9	78	11
節外性辺縁帯B細胞リンパ腫	7	86	43

(文献[4]より引用改変)